Enhanced therapeutic potential of a microdystrophin with an extended C-terminal domain

Steven Foltz[1], Randolph Qian[1], Jason Yang[1], Kirk Elliott[1], Hannah Jasick[1], Benjamin P. Heithoff[1], Jared B. Smith[1], George Dickson[2], Ye Liu[1], and Olivier Danos[1]

[1]Gene Therapy Research, REGENXBIO Inc., Rockville, MD; [2]School of Life and Environmental Sciences, Royal Holloway – University of London, Surrey, UK

Introduction

Gene therapy is emerging as a therapeutic option for patients with Duchenne muscular dystrophy (DMD), caused by loss of functional dystrophin protein. The dystrophin coding sequence exceeds the packaging limit of adeno-associated virus (AAV), the preferred delivery vector for muscle gene therapy. Several truncated, AAV-compatible "microdystrophins" have been designed and shown to retain many, though not all, functional features of the full-length protein. Microdystrophins differ from one another according to their combinations of hinges and spectrin-like repeats and the inclusion of dystrophin functional domains. While several microdystrophins have advanced to the clinic, an optimal microdystrophin configuration has not been empirically determined.

The highly conserved dystrophin C-Terminal domain (CT) is absent from all but one clinical-stage microdystrophin (RGX-202, REGENXBIO), despite evidence that this region recruits important signaling proteins to the sarcolemma and prevents force loss following damaging muscle contraction. To test whether the CT contributes to μDys functionality we produced AAV vectors encoding versions of μDys without ("μDysCT48") or with ("μDysCT194") an extended piece of the CT. We found that μDysCT194 is maintained at higher levels in transduced muscles, recruits the dystrophin-associated protein complex more effectively to the sarcolemma, and provides improved histopathological benefit in dystrophin-deficient *mdx* mice. A protocol of 20 consecutive lengthening contractions reduced force to 18.3% of initial value in *mdx* and 56.6% in WT controls. In *mdx* mice expressing μDysCT48, a reduction to 34.4% was measured, whereas in μDysCT194 treated animals, force drop was limited to 49.4%. To survey contraction-induced muscle damage, mice were injected with myofiber impermeant Evans blue dye prior to lengthening contraction. In *mdx* Vehicle mice, 22.5% of fibers were dye-positive following ECC indicating significant cell membrane compromise, which was attenuated more effectively by μDysCT194 than μDysCT48 (4.6% vs. 11.2%, respectively). Our results indicate that incorporation of the CT enhances microdystrophin function.

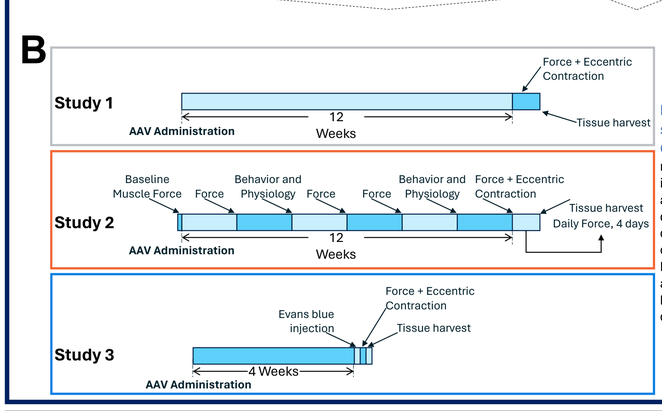

Figure 1. μDys transgenes and studies used to evaluate benefit of CT domain. (A) Schematic representation of μDys transgenes, identical aside from C-Terminal length, aligned to full-length *DMD* gene and dystrophin structural domains. (B) Study design for 3 *in vivo* studies directly comparing the μDys proteins from (A). Boxes outlining each subsequent figure are color-matched to the boxes shown here based on the Study from which the data were obtained.

Materials and Methods

AAV Vectors. Transgene cassettes encoding μDys were packaged into AAVhu32 and included the muscle-specific Spc5-12 promoter. Vectors were administered to 5-week-old *mdx* mice by tail vein injection at a dose of $5x10^{13}$ GC/kg (unless otherwise noted).

In Vitro *Force.* Left and right extensor digitorum longus (EDL) muscles were removed sequentially from each mouse and immersed in individual oxygenated baths containing Ringer's solution (pH 7.4) at 25°C. Maximal force was measured with each muscle held at 10 mN. After force measurement, the right EDL was subjected to a lengthening contraction {eccentric contraction (ECC)} protocol, which was used to induce injury to the muscle. The right EDL muscle was lengthened or stretched by 10% above the optimal length (L_o) and stimulated 5 times separated by 4-minute rest intervals.

In vivo *Force*. Mouse hindlimbs were pinned at the knee and feet were affixed to a plate attached to a force transducer. Contraction was elicited by tibial nerve stimulation. Eccentric contraction (ECC) was achieved by rotation of the foot at the ankle to lengthen the plantarflexors with simultaneous tibial nerve stimulation.

Evans blue injection and analysis. Evans blue dye was formulated as 1% w/v solution in isotonic saline solution and injected at 0.5% bodyweight. ECC was performed 1 day post Evans blue injection, and tissues were harvested 1 day post ECC

***Grip strength, Treadmill and Open Field Activity*.** Animals were acclimated to the grip strength meter for 2 consecutive days prior to testing. The testing day consisted of five recorded forelimb pulls separated by 30 seconds each. After establishing grip, animals were pulled by the tail away from the grip strength meter while maintaining the body parallel to the benchtop surface. Mice were weighed prior to testing to normalize force measurement to body weight. The highest value of the five pulls was reported for each animal. Exercise capacity was determined via incentivized treadmill running. Mice were placed in lanes on a treadmill with shock pad at the end of the lane in the direction of belt motion. Belt speed was gradually increased. Fatigue distance is defined as the length (in meters) run before the mouse spent >30s consecutively in the half of the lane closest to the shock pad. Exhaustion distance is defined as the length (in meters) run before the mouse spent >5 consecutive seconds on the shock pad. Open field activity was assessed as a complementary measurement of voluntary activity. Mice were placed in a square chamber and motion was captured using a ceiling-mounted camera (Noldus). Movement parameters were classified according to the type of motion (e.g. total distance traveled is a 'movement' parameter and time spent in the center of the chamber is a 'location' parameter).

Immunofluorescence. 10 μm cryosections were incubated with primary antibodies against dystrophin/μDys (DSHB, 1:1000; Leica, 1:50), syntrophin-α1 (Alomone, 1:200), α-Dystrobrevin (SantaCruz, 1:200), or embryonic myosin heavy chain (eMyHC) (DSHB, 1:10), counterstained with anti-laminin (Sigma, 1:400) overnight and detected with fluorescent secondary antibodies. Whole tissue 20x tiled images were acquired on a Zeiss AxioScan 7 slide scanner.

Histology. Hematoxylin and eosin staining was performed on dry cryosections with Mayer's hematoxylin and 1% alcoholic eosin (Electron Microscopy Sciences). Sirius red (Abcam) staining was performed according to the manufacturer's protocol. Sections were dehydrated, cleared, and coverslips were mounted with Permount (Fisher) mounting medium.

DNA/RNA Extraction and ddPCR. Total RNA and DNA were extracted from tissues using the Kingfisher Apex via the MagMAX mirVana Total RNA and MagMAX DNA multi-Sample Ultra 2.0 kits (Thermo). μDys-specific primers/probes were used to measure μDys expression and vector genome copies. RNA was converted to cDNA using the Maxima First Strand cDNA Synthesis Kit (Thermo). values were normalized by TATA binding protein (*Tbp*) copies, and vector genomes were normalized by glucagon copies.

Capillary Electrophoresis. Total protein was extracted from gastrocnemius, quadriceps, and EDL skeletal muscles in SDS/Tris buffer. 3μg of protein per sample were loaded onto plates for analysis by capillary electrophoresis (Jess, bio-techne). Purified His-tagged μDysCT194 was generated by LakePharma. Dystrophin/μDys were detected with a primary antibody recognizing Hinge 1 (DSHB, 1:50) and HRP-conjugated anti-mouse secondary antibody.

Quantification and statistics. Fluorescent intensity was quantified within laminin$^+$ areas for syntrophin and dystrobrevin. The percentage of dystrophin-positive fibers was determined using HALO software. eMyHC$^+$ cells were scored manually in ImageJ and normalized to tissue cross-sectional area. Sirius red- and Evans blue-positive areas were quantified in ImageJ by adjusting the image color threshold and measuring stain-positive area. Total μDys protein levels are normalized to wild-type, full-length dystrophin levels (where the average dystrophin level of all wild-type controls is set to 1). Bar graphs show mean ± SEM and were analyzed by either Student's t-test or one-way ANOVA with Holm-Sidak multiple comparisons correction. For correlative analyses, simple linear regression was performed followed by calculation of Pearson correlation coefficient. A value of $p < 0.05$ was considered statistically significant for all tests.

Results

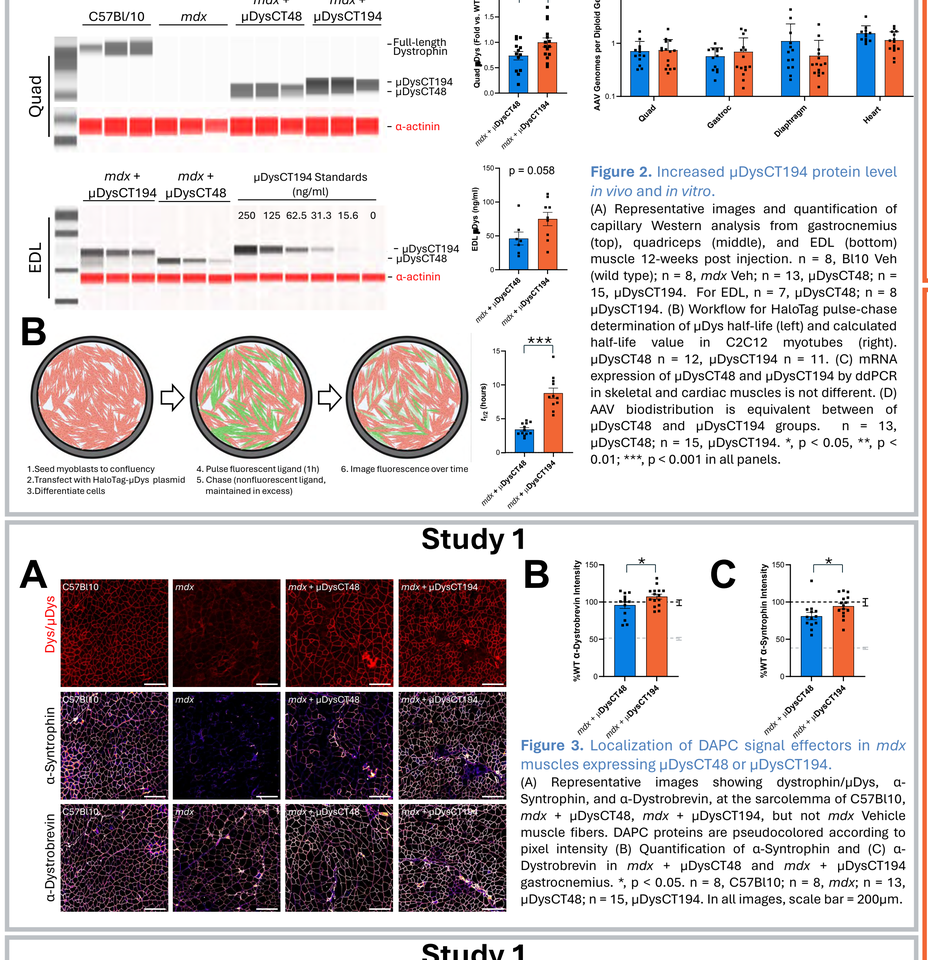

Figure 2. Increased μDysCT194 protein level *in vivo* and *in vitro*.
(A) Representative images and quantification of capillary Western analysis from gastrocnemius (top), quadriceps (middle), and EDL (bottom) muscle 12-weeks post injection. n = 8, Bl10 Veh (wild type); n = 8, *mdx* Veh; n = 13, μDysCT48; n = 15, μDysCT194. For EDL, n = 7, μDysCT48; n = 8 μDysCT194. (B) Workflow for HaloTag pulse-chase determination of μDys half-life (left) and calculated half-life value in C2C12 myotubes (right). μDysCT48 n = 12, μDysCT194 n = 11. (C) mRNA expression of μDysCT48 and μDysCT194 by ddPCR in skeletal and cardiac muscles is not different. (D) AAV biodistribution is equivalent between of μDysCT48 and μDysCT194 groups. n = 13, μDysCT48; n = 15, μDysCT194. *, $p < 0.05$, **, $p < 0.01$; ***, $p < 0.001$ in all panels.

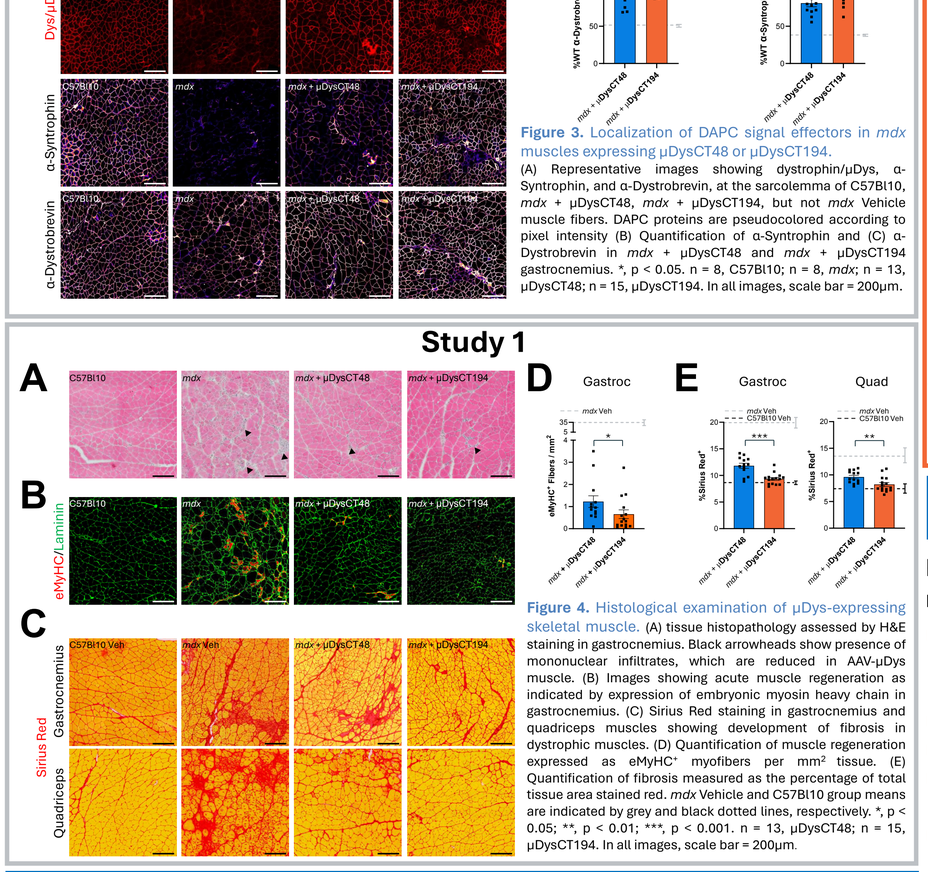

Figure 3. Localization of DAPC signal effectors in *mdx* muscles expressing μDysCT48 or μDysCT194.
(A) Representative images showing dystrophin/μDys, α-Syntrophin, and α-Dystrobrevin, at the sarcolemma of C57Bl10, *mdx* + μDysCT48, *mdx* + μDysCT194, but not *mdx* Vehicle muscle fibers. DAPC proteins are pseudocolored according to pixel intensity (B) Quantification of α-Syntrophin and (C) α-Dystrobrevin in *mdx* + μDysCT48 and *mdx* + μDysCT194 gastrocnemius. *, $p < 0.05$. n = 8, C57Bl10; n = 8, *mdx*; n = 13, μDysCT48; n = 15, μDysCT194. In all images, scale bar = 200μm.

Figure 4. Histological examination of μDys-expressing skeletal muscle. (A) tissue histopathology assessed by H&E staining in gastrocnemius. Black arrowheads show presence of mononuclear infiltrates, which are reduced in AAV-μDys muscle. (B) Images showing acute muscle regeneration as indicated by expression of embryonic myosin heavy chain in gastrocnemius. (C) Sirius Red staining in gastrocnemius and quadriceps muscles showing development of fibrosis in dystrophic muscles. (D) Quantification of muscle regeneration expressed as eMyHC$^+$ myofibers per mm^2 tissue. (E) Quantification of fibrosis measured as the percentage of total tissue area stained red. *mdx* Vehicle and C57Bl10 group means are indicated by grey and black dotted lines, respectively. *, $p < 0.05$; **, $p < 0.01$; ***, $p < 0.001$. n = 13, μDysCT48; n = 15, μDysCT194. In all images, scale bar = 200μm.

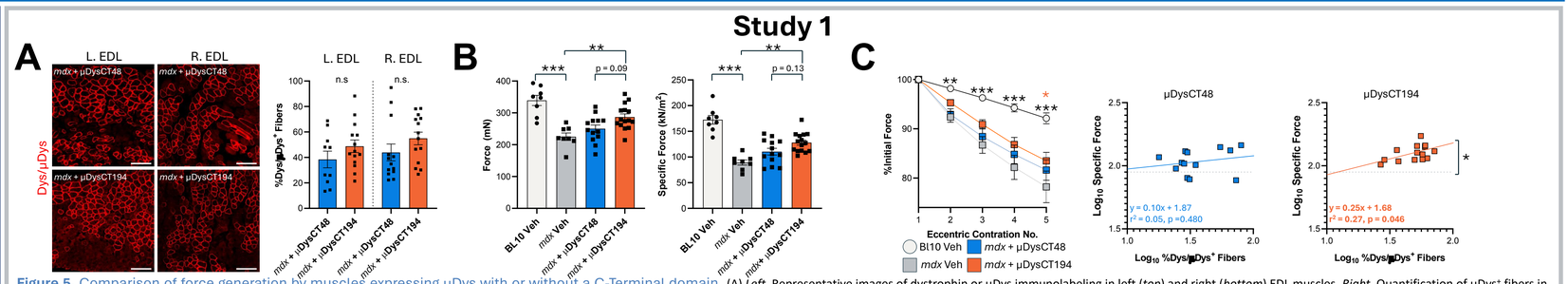

Figure 5. Comparison of force generation by muscles expressing μDys with or without a C-Terminal domain. (A) *Left,* Representative images of dystrophin or μDys immunolabeling in left (*top*) and right (*bottom*) EDL muscles. *Right,* Quantification of μDys$^+$ fibers in left and right EDL muscle from transverse tissue sections taken at several depths through the muscle. (B) EDL maximal and specific force measured *ex vivo* at study termination. (C) *Left*, Force drop following repeated eccentric contractions. Asterisks denote statistical significance vs. *mdx* Vehicle group. *Right,* Comparison of percentages of *mdx* muscle fibers expressing dystrophin/μDys and specific force generation in EDL. Gray dotted line marks average specific force for *mdx* Vehicle group. Asterisk denotes a significantly non-zero slope for μDysCT194. Pearson correlation coefficients and associated p-values are also shown. *, $p < 0.05$; **, $p < 0.01$; ***, $p < 0.001$. n = 8, C57Bl10; n = 8, *mdx*; n = 13, μDysCT48; n = 15, μDysCT194. n = 13, μDysCT48; n = 15, μDysCT194.

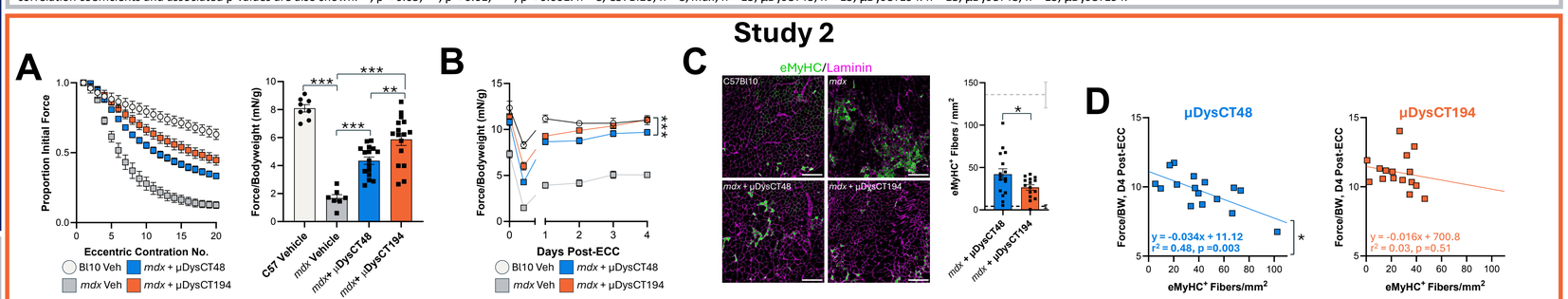

Figure 6. Recovery from eccentric exercise. (A) *Left,* force, expressed as a percentage of initial force, following a series of eccentric contractions *in vivo* 12-weeks post-dosing. *Right,* maximal force generated by plantar flexors following 20 eccentric contractions, normalized to bodyweight. (B) Bodyweight-normalized maximal force generated by plantar flexors immediately before, immediately after, and daily for 4 days post eccentric contraction protocol. (C) *Left,* representative images and *right* quantification of eMyHC$^+$ muscle fibers 7 days after a protocol of 20 eccentric contractions in plantar flexor muscles. (D) Bodyweight-normalized plantar flexion force represented as a function of eMyHC content in muscles 7 days post-ECC. **, $p < 0.01$; ***, $p < 0.001$.

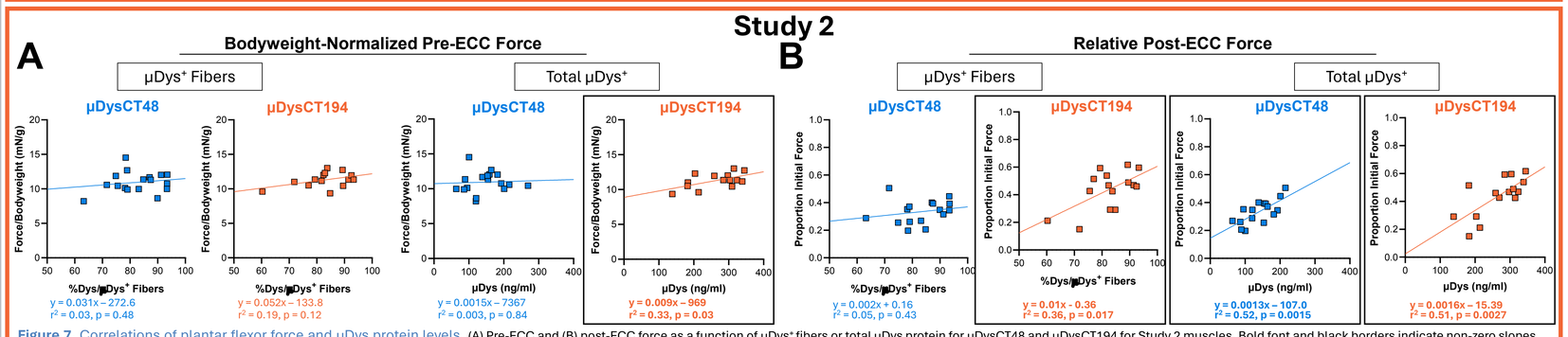

Figure 7. Correlations of plantar flexor force and μDys protein levels. (A) Pre-ECC and (B) post-ECC force as a function of μDys$^+$ fibers or total μDys protein for μDysCT48 and μDysCT194 for Study 2 muscles. Bold font and black borders indicate non-zero slopes for lines of best fit and statistically significant r^2 values. μDys$^+$ fibers were measured in the right gastrocnemius muscle, which was subjected to the ECC protocol. Total μDys protein was measured in the left gastrocnemius, which was ECC-naïve. n = 16, μDysCT48; n = 16, μDysCT194.

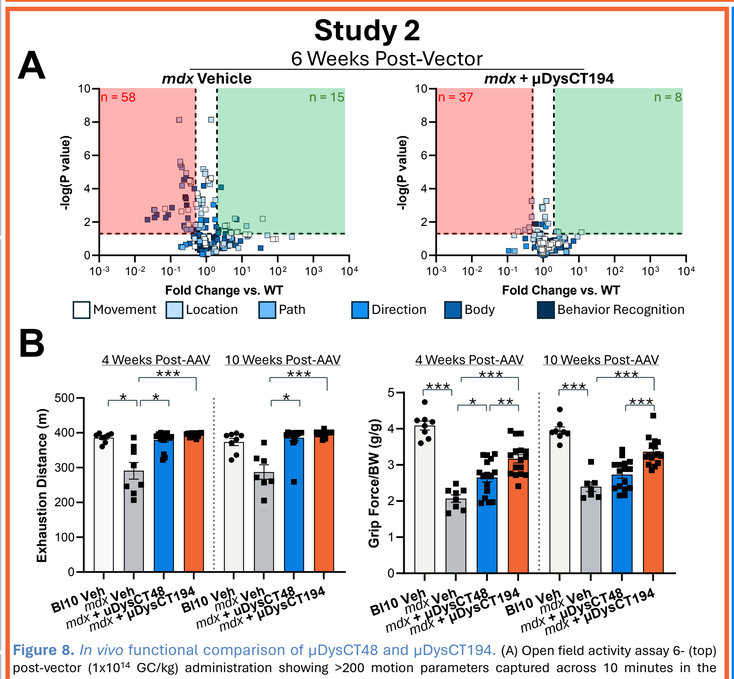

Figure 8. *In vivo* functional comparison of μDysCT48 and μDysCT194. (A) Open field activity assay 6- (top) post-vector ($1x10^{14}$ GC/kg) administration showing >200 motion parameters captured across 10 minutes in the chamber per mouse. Data are represented as Volcano plots, with the change in the recorded value relative to WT controls shown on the x-axis and the p-value associated with that change shown on the y-axis. Dotted lines show a p-value < 0.05 and relative parameter change values (relative to WT) <0.5 and >2.0. Red boxes show activities significantly reduced relative to WT, while green boxes show activities significantly increased. (B) *Left,* Distance to exhaustion on an accelerating treadmill test 4- and 10-weeks post-dosing. *Right,* Grip strength measurements taken 4- and 10-weeks post-dosing, normalized to mouse bodyweight. n = 8, C57Bl10; n = 7-8, mdx; n = 16, μDysCT48; n = 16, μDysCT194. In all panels, *, $p < 0.05$; **, $p < 0.01$; ***, $p < 0.001$.

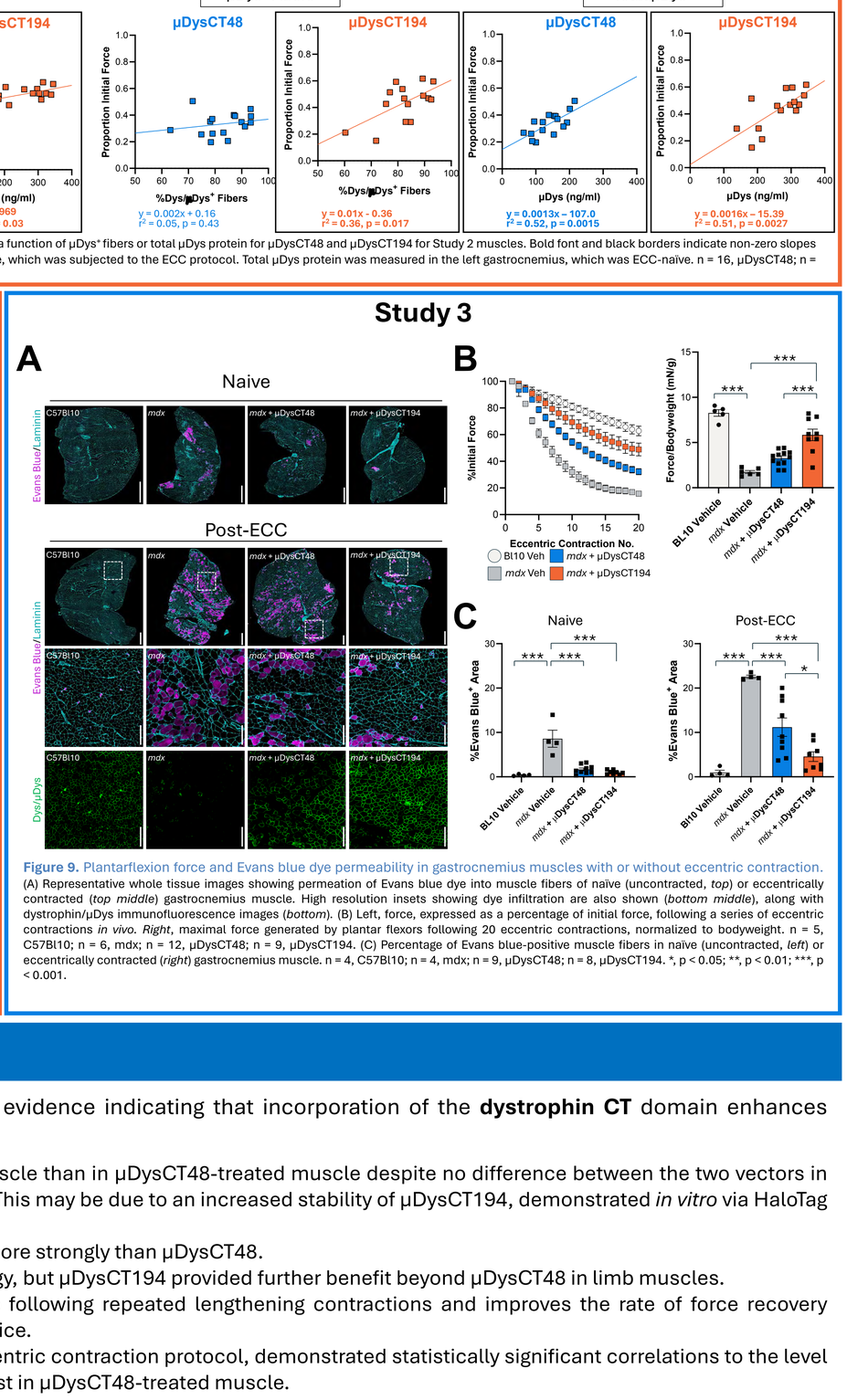

Figure 9. Plantarflexion force and Evans blue dye permeability in gastrocnemius muscles with or without eccentric contraction.
(A) Representative whole tissue images showing permeation of Evans blue dye into muscle fibers of naïve (uncontracted, *top*) or eccentrically contracted (*top middle*) gastrocnemius muscle. High resolution insets showing dye infiltration are also shown (*bottom middle*), along with dystrophin/μDys immunofluorescence images (*bottom*). (B) Left, force, expressed as a percentage of initial force, following a series of eccentric contractions *in vivo*. *Right*, maximal force generated by plantar flexors following 20 eccentric contractions, normalized to bodyweight. n = 5, C57Bl10; n = 6, mdx; n = 12, μDysCT48; n = 9, μDysCT194. (C) Percentage of Evans blue-positive muscle fibers in naïve (uncontracted, *left*) or eccentrically contracted (*right*) gastrocnemius muscle. n = 4, C57Bl10; n = 4, mdx; n = 9, μDysCT48; n = 8, μDysCT194. *, $p < 0.05$; **, $p < 0.01$; ***, $p < 0.001$.

Discussion and Conclusions

Results from these preclinical studies provide several lines of evidence indicating that incorporation of the **dystrophin CT** domain enhances microdystrophin function.

- Steady-state μDys protein level is higher in μDysCT194-treated muscle than in μDysCT48-treated muscle despite no difference between the two vectors in terms of vector biodistribution to muscle or μDys RNA expression. This may be due to an increased stability of μDysCT194, demonstrated *in vitro* via HaloTag pulse-chase.
- μDysCT194 restores DAPC signaling effectors to the sarcolemma more strongly than μDysCT48.
- Both μDys led to strong improvements in *mdx* muscle histopathology, but μDysCT194 provided further benefit beyond μDysCT48 in limb muscles.
- μDysCT194 increases muscle force and resistance to force drop following repeated lengthening contractions and improves the rate of force recovery following an eccentric contraction muscle-injury protocol in *mdx* mice.
- Bodyweight-normalized muscle force, either before or after an eccentric contraction protocol, demonstrated statistically significant correlations to the level of μDysCT194 protein expressed in muscle, some off which were lost in μDysCT48-treated muscle.
- μDysCT194 increases voluntary and incentivized activity in *mdx* mice.
- μDysCT194 substantially decreases basal myofiber permeability to Evans blue dye compared to *mdx* Vehicle mice and protects against increased permeability observed following a series of eccentric muscle contractions.
- RGX-202, an investigational μDys therapy for DMD featuring μDysCT194 , has entered clinical trials (AFFINITY DUCHENNE®, NCT05693142).

Acknowledgements

We acknowledge the REGENXBIO Vector Core team for production of vectors used in this study. Animal Study 1 was conducted at AGADA Biosciences Inc., led by Dr. Diogo Poroca under the supervision of Dr. Pia Elustondo. Myologica LLC provided training and assisted in experimental protocol development for *in vivo* force assays.